ORIGINAL ARTICLE

lajss.org
Latin American Journal of Solids and Structures

www.lajss.org

Experimental study on pulse shaping techniques of large diameter SHPB apparatus for concrete

Jiangbo Wang[a], Wenfeng Li[a], Lizhi Xu[a], Zhonghua Du[a], Guangfa Gao[a]*

[a] School of Mechanical Engineering, Nanjing University of Science and Technology, Nanjing, Jiangsu 210094, P.R. China.
E-mail: wjbo1993@163.com, liwenfenger@163.com, xulznjust@163.com, duzhonghua@aliyun.com, gfgao@ustc.edu.cn.

* Corresponding author

https://doi.org/10.1590/1679-78256268

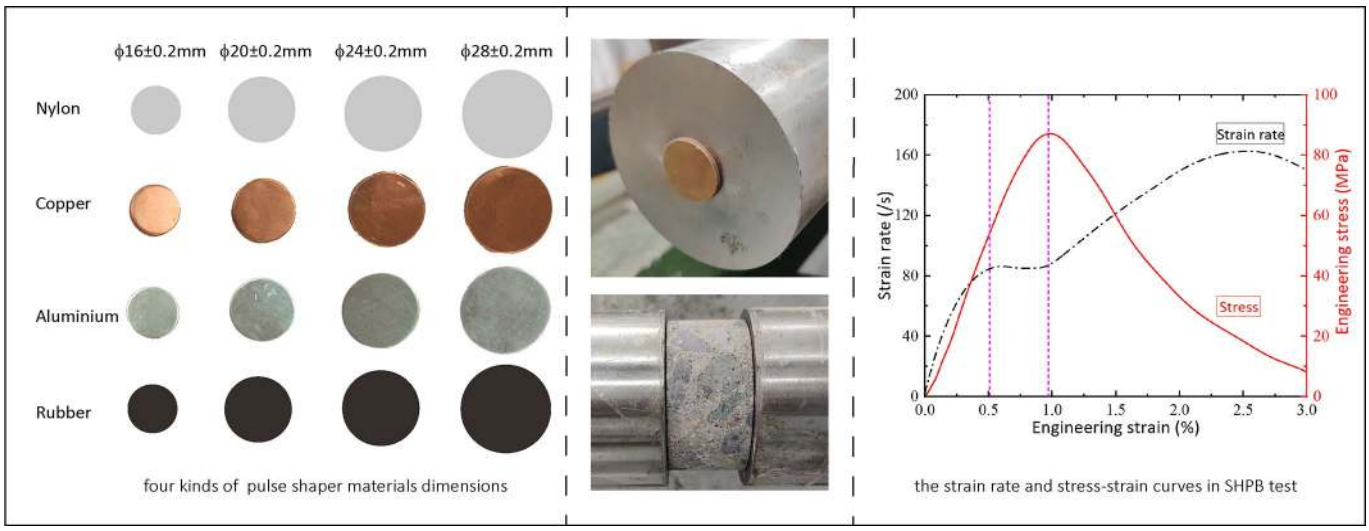
ABSTRACT

The constant strain rate loading and dynamic stress equilibrium are prerequisites for ensuring the experimental data of the Split Hopkinson Pressure Bar (SHPB). In order to achieve this requirement, a proper pulse shaper dimensions were used in the experiment. For this purpose, the pulse shaper diameter, thickness and strength and the strike bar length and its velocity on the incident pulse are studied by Ø80mm SHPB apparatus. Then, the parameters affecting the two key inflection points and three loading areas of the incident pulse are discussed. In addition, the improved methods for two typical non-constant strain rate waveforms for the concrete experiments are obtained based on the regular pulse shaping. Moreover, SHPB experiments are conducted for concrete by employing different pulse shaper dimensions. The results show that more valid data can be obtained by employing the pulse shaper with large thickness when the strain rate is non-constant during the experiment. The conclusions and method provide guidance for selecting pulse shaper for concrete SHPB experiments.

Keywords

Pulse Shaper; Incident pulse; Constant strain rate; SHPB, Concrete.

Graphical Abstract



Received: September 19, 2020. In Revised Form: December 29, 2020. Accepted: December 29, 2020. Available online: January 07, 2021.
https://doi.org/10.1590/1679-78256268

Latin American Journal of Solids and Structures. ISSN 1679-7825. Copyright © 2021. This is an Open Access article distributed under the terms of the Creative Commons Attribution License, which permits unrestricted use, distribution, and reproduction in any medium, provided the original work is properly cited.

1 Introduction

Concrete and rock materials have been widely applied in the military protection field for their excellent characteristics, such as high compressive strength, low density and relatively lower cost. In the field, defensive constructions made of concrete and rock materials usually subject to shock and explosion dynamic loads, so it is very significant to understand their dynamic mechanical properties for their effective application. It is well known that split-Hopkinson pressure bar (SHPB) or Kolsky bar (Kolsky, 1949) is one of the most commonly used experimental equipment to investigate the dynamic mechanical properties of materials. Based on the basic principle of SHPB (Chen et al., 2002), it is necessary to ensure the dynamic stress equilibrium and the constant strain rate to obtain valid results. Since concrete and rock behave small failure strain, the shape of the incident wave has to be adjusted to meet conditions of the dynamic stress equilibrium and the constant strain rate. Now, the research shows that the main technologies of modifying the incident pulse include adjusting the strike bar shape (Lok et al., 2002; Baranowski et al., 2013), using pre-loading bar technology (Parry et al., 1995) and pulse shaper technology (Chen et al., 2003). Since the first and second methods have many drawbacks, such as difficulty in processing the shape of the strike bar and realizing constant strain rate loading, so the pulse shaper has become the most widely used technology. Its principle is to place a sheet of soft material between the strike bar and incident bar. By selecting the appropriate material and size, the conditions for reducing the incident wave oscillation, achieving dynamic stress equilibrium and constant strain rate loading in the SHPB experiment can be realized.

Most studies on pulse shaping techniques focus on small diameter SHPB equipment. Frew et al. (2002, 2005) obtained an analysis model of pulse shaper for SHPB equipment with diameters of 12.7mm and 19.3mm based on the material volume incompressibility and uniform deformation theory. Naghdabadi et al. (2012) conducted experimental research and numerical simulation on the influence of shaper on incident pulse based on a 12.8mm SHPB apparatus, besides, qualitative selection criteria of shaper dimensions for small diameter SHPB test was obtained. Panowicz et al. (2018) used numerical simulation to analyze the influence of square, circular, cross, star and circular shapers on the incident pulse. Other researchers (Hwang et al., 2005; Peroni et al., 2006; Tang et al., 2008; Li et al., 2000) simply introduced the selection of shaper material and size for small diameter SHPB test of a specific material. Whether the conclusion of pulse shaper technology from small-diameter SHPB test can be perfectly applied to the large-diameter SHPB test, it should be further verified.

In order to study the dynamic compression properties of concrete materials, Bagher Shemirani et al. (2016) experimented pulse shapers with thicknesses of 1 and 2 mm by using C10200 copper. The effects of pulse shaper on the shape, compressive strength, elastic modulus, toughness and damage behavior of concrete is analyzed. It is concluded that for different strain rates, the cross-sectional area and thickness of the shaper are proportional to the velocity of the strike bar. Guo et al. (2017) used two circular brass composite pulse shapers with diameters of 6-10 mm and 20-38 mm respectively to conduct dynamic compression experiments on C60, C80 and C110 concrete. The smaller diameter shaper is used to enhance the full surface contact between the specimen and the loading bar, and then the larger shaper deforms to increase the incident wave sharply, causing the specimen to be loaded into a failed state. Heard et al. (2014) used a ring shaper in the SHPB experiment of concrete materials to improve the dynamic stress equilibrium and constant strain rate deformation of the specimen. In addition, the shaper material in the SHPB experiment for concrete materials also includes rubber (Chen et al., 2013; Ma et al., 2019) and brass(Yang et al., 2015; Su et al., 2014; Xin et al., 2013).

In the present paper, five groups of experiments are performed with Ø80 mm SHPB apparatus to discuss the influence factors (diameter, thickness, pulse shaper length and its strength, strike bar velocity) on the incident pulse. Four materials were used in each group experiment, including copper, aluminum, nylon and rubber. The energy absorption status of four shaper materials was analyzed, and then the improved methods for two typical non-constant strain rate loading waveforms in the concrete SHPB experiment were obtained. Finally, SHPB experiments of concrete with different pulse shaper dimensions is performed according to the improved method. The effect of pulse shaper dimensions on the dynamic stress equilibrium and constant strain rate is analyzed, and the selection method of the pulse shaper is discussed for concrete experiment.

2 Experimental procedure

2.1 SHPB experimental apparatus

An SHPB apparatus with a diameter of 80 mm is used in the experiment as shown in **Fig. 1**. The apparatus consists of a launcher, strike bar, incident bar, transmission bar, energy absorption device and data acquisition system, and the geometric and materials parameters of the bar are listed in **Table 1**. The strike bar is launched by a gas gun to impact the

incident bar and an elastic compressive pulse is generated. According to the one-dimensional elastic wave theory, transmission and reflection phenomena will be generated on the contact surface between the specimen and bars. The reflected pulse and incident pulse is recorded by a diametrically-opposed pair of strain gauges attached to the middle position of the incident bar, while the transmitted pulse is measured by another pair of diametrically-opposed strain gauges at the mid-point of the transmission bar. From the incident, reflected and transmitted strain signals detected by the strain gauges on the incident/transmission bars, the strain rate($\dot{\varepsilon}$), strain(ε) and stress(σ) of the specimen can be calculated by the following equations:

$$\begin{cases} \dot{\varepsilon}(t) = -2\dfrac{C_b}{L_S}\varepsilon_r(t) \\ \varepsilon(t) = -2\dfrac{C_b}{L_S}\int_0^t \varepsilon_r(t)\,dt \\ \sigma(t) = \dfrac{A_b}{A_S}E_b\varepsilon_t(t) \end{cases} \tag{1}$$

where A_b is the cross-sectional area of the bar, A_S and L_S are the cross-sectional area and length of the specimen, C_b and E_b are elastic wave velocity and Young's modulus in the bars, respectively; and $\varepsilon_r(t)$ and $\varepsilon_t(t)$ are the reflected and transmitted strain, respectively.

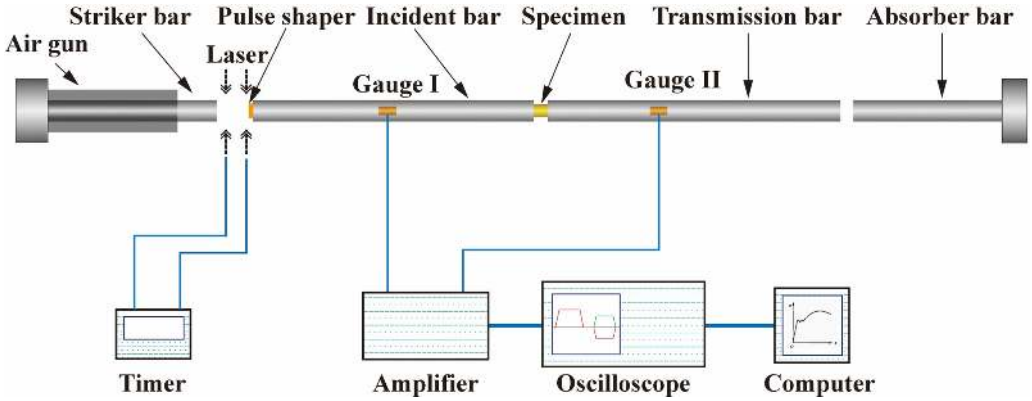


Figure 1 Schematic of the SHPB experiment system

Table 1 Specifications of the SHPB experimental system

Bar parameter (40Cr Steel)	Geometric parameter		Physical parameters			
	Diameter(mm)	Length (mm)	*E*(GPa)	*ρ* (g/cm³)	v	C_b (m/s)
Strike bar	80	500/1000	210	7.85	0.3	5210
Incident bar		6000				
Transmission bar		4000				

Note: *E* is the Young's modulus of the bar; *ρ*, v and C_b are the density, Poisson's ratio and elastic wave velocity in the bars, respectively.

2.2 Experimental arrangement

In this investigation, the copper, aluminum, nylon and rubber materials were used to study the effects of pulse shaper on the incident pulse shape, including the pulse shaper diameter and thickness, as well as the strike bar lengths and its velocities. A series of SHPB experiments were performed on every shaper material to study the effect of diameters, thicknesses, and velocities on the incident pulse, and the specific experimental scheme is shown in **Table 2**. In order to ensure the accuracy of the experiment data, three repetitive experiments were conducted on every type of pulse shapers.

The compressive strength of pulse shaper material is also an important factor affecting the incident pulse. **Fig.2** shows the stress-strain curves of four materials under quasi-static uniaxial compression. The samples dimensions are 10mm in diameter and 10mm in length consists of 10 discs with the size of Ø10×1 mm stacked together. It shows that the copper, aluminum and nylon materials have obvious yield stages, and the yield strength decreases in turn. The stress-strain curve of rubber material is approximately linear growth without an obvious yield stage.

Table 2 Experimental scheme design

Geometric and material parameters of pulse shaper			Strike bar parameters	
materials	**Diameter (mm)**	**Thickness (mm)**	**Length (mm)**	**Velocity (m/s)**
Copper/Aluminum	16/20/24/28	1.0	1000	9
Nylon/ Rubber				7
Copper	20	0.6/0.8/1.0/1.2		9
Aluminum		0.8/1.0/1.2/1.5		
Nylon		1.0/1.2/1.5/2.0		7
Rubber		0.8/1.0/1.5/2.0		
Copper		1.0	500/1000	6/9/12
Aluminum		1.0		9

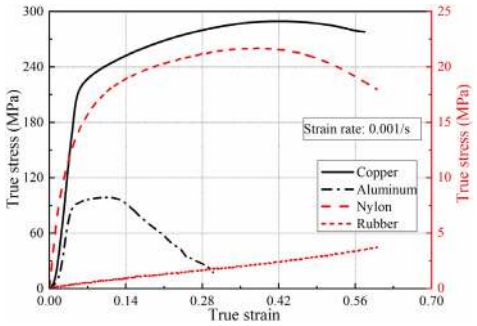


Figure 2 Compressive stress-strain curves of four materials with sample dimensionsØ10×10mm

2.3 Data processing method

Fig.3(a) shows the incident pulse of the SHPB experiments with or without copper pulse shaper. Under the same experimental conditions, the three experiments with pulse shaper have in good agreement, which indicates that the experimental data are accurate. To show the most essential feature of the incident pulse without pulse shaper, it was smoothed as shown in the green dotted line in **Fig. 3(a)**.

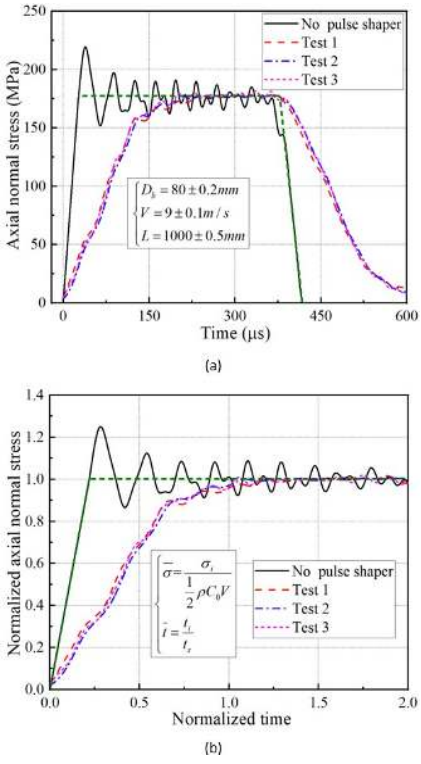


Figure 3 Incident pulse with shaper dimensions of Ø20×1mm for (a) without pulse shaper and waveform repeatability; (b) correction-normalization curve.

According to the wave theory, the abscissa and ordinate of the incident pulse were normalized, i.e., the longitudinal coordinates are divided by the theoretical stress value, and the abscissa time is divided by the theoretical pulse duration (**Eqs. (2)** and **(3)**).

$$\bar{\sigma} = \frac{\sigma_i}{\frac{1}{2}\rho C_0 V} \tag{2}$$

$$\bar{t} = \frac{t_i}{t_s} \tag{3}$$

where $\bar{\sigma}$ is the normalized stress, σ_i the incident pulse stress, V is the strike bar velocity, $\bar{t}$ is the normalized time, t_i is the incident pulse time. However, in the process of normalizing the incident pulse, it is found that the average peak pressure corresponding to the incident waveform fluctuates within 5% of the theoretical value. The main reason is that the sensitivity of the resistance strain gauge and the strike bar velocity fluctuate. In this paper, the influence of pulse shaper on the unloading part of incident pulse is not considered. Therefore, the correction-normalization curve and the incident pulse without unloading part were obtained as shown in **Fig.3 (b).**

3 Results and discussion

Fig. 4 demonstrates the results of incident pulse with or without a pulse shaper when the strike bar is 1m in length and 9m/s in velocity. According to **Fig.4**, the rise time of the incident pulse is increased when a pulse shaper is employed. In addition, when a pulse shaper of suitable dimensions is used, the high-frequency oscillation wave can be filtered out to minimize the wave dispersion and meet the assumption of dynamic stress uniformity of SHPB. The incident pulse is generally trapezoidal without a pulse shaper in SHPB experiment. The function of pulse shaper is to absorb the energy through plastic deformation to change the incident pulse. By observing the incident pulse in **Fig.4**, it is found that the incident pulse with pulse shaper can be divided into three parts (Naghdabadi et al., 2012) and two key inflection points (ignore the unloading part of the waveform):

I. The elastic deformation loading part of pulse shaper during the impact loading process of the strike bar.

II. The plastic deformation loading part of pulse shaper during the impact loading process of the strike bar.

III. The remaining incident wave continues to be loaded. Since the strike bar length is the same, the duration of the loading pulse is constant. After the pulse shaper is completely plastically deformed, the subsequent loading is rigid loading, which is the same as the shapeless waveform of the high-frequency shock wave.

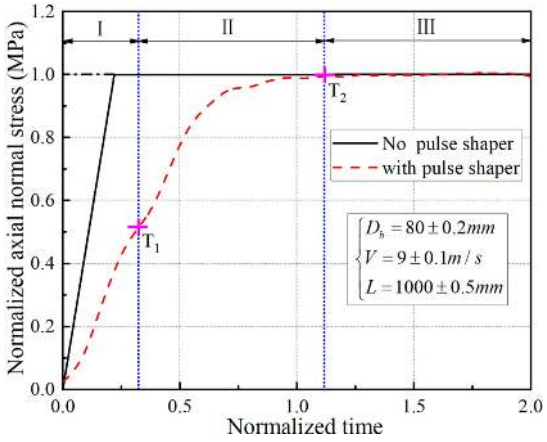


Figure 4 Typical incident pulse with or without pulse shaper

3.1 Effect of pulse shaper diameter

Fig. 5 shows the results of the pulse shaper with different diameters on the incident pulse in the SHPB experiment. The pulse shaper thickness, the strike bar length and its velocity are 1mm, 1000mm and 9m/s, respectively. As shown in the figure, for metal pulse shapers (copper and aluminum), the inflection point T_1 of the incident waveform increases with the pulse

shaper diameter increases, and the duration of elastic loading part I also increases. For different diameters of non-metallic pulse shapers (nylon and rubber), the inflection point T_1 is approximately the same. However, the duration of elastic loading I of nylon pulse shaper remains unchanged. And the waveforms of the rubber shaper with diameters of 24mm and 28mm are almost completely coincident, which means that the rubber pulse shaper has a certain diameter limitation. In other words, when the pulse shaper diameter exceeds the limit diameter, the incident waveform does not change accordingly.

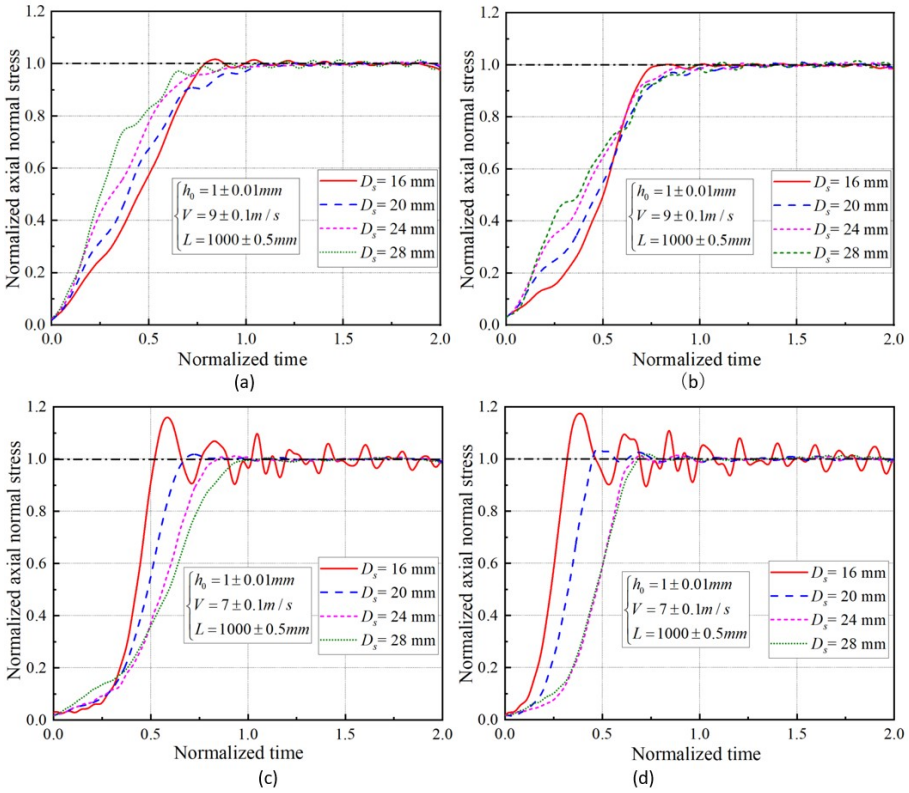


Figure 5 Incident wave curve of shaper with different diameters in SHPB experiment (a) copper (b) aluminum (c) nylon (d) rubber.

The influence of the pulse shaper diameter on the inflection point T_1 is explained in terms of shaper strain. For the incompressible material hypothesis, volume conservation gives

$$a_0 h_0 = a(t)h(t) \tag{4}$$

where a_0 is the original and $a(t)$ and $h(t)$ are the current cross-sectional area and thickness of the pulse shapers. The axial engineering strain in the pulse shaper during compression is given by

$$\varepsilon_p(t) = \frac{h_0 - h(t)}{h_0} \tag{5}$$

From **Eqs. (4)** and **(5)**, the current cross-sectional area of the pulse shaper can be expressed by the original cross-sectional area and axial engineering strain.

$$a(t) = \frac{a_0}{1 - \varepsilon_p(t)} \tag{6}$$

The axial force is equal in the process of impact, it can be obtained

$$T(t) = \sigma_p(t)a(t) = \sigma_i(t)A_b = \sigma_{st}(t)A_b \tag{7}$$

where $\sigma_p(t)$ is the current axial stress in the pulse shaper, $\sigma_i(t)$ and $\sigma_{st}(t)$ are the compressive stresses in the incident and strike bar. Thus, compressive stress in the incident bar is

$$\sigma_i(t)=\frac{\sigma_p(t)a(t)}{A_b} \tag{8}$$

For the first inflection point T_1(i.e., where is the pulse shaper reaching yield strength during compression), $\sigma_p(t)$ in **Eq. (8)** is the pulse shaper material yield strength. For the different diameters of the pulse shapers, $\sigma_p(t)$ and $\varepsilon_p(t)$ are the constants, and from **Eqs. (6)** and **(8)**, it is found that the inflection point T_1 gradually increases as the pulse shaper diameter increases in the incident pulse. When the pulse shaper material is metal, the diameter changing has no obvious effect on the rising edge end T_2 of the incident pulse. However, when non-metallic materials as the pulse shapers, the rising edge T_2 moves to the right as the pulse shaper diameter increases in the incident pulse.

3.2 Effect of pulse shaper thickness

To further analyze the effects of pulse shaper thicknesses on the waveform, a series of experiments with different thicknesses were carried out. **Fig.6** is the results of the pulse shaper with different thicknesses on the incident pulse in the SHPB experiment. For the metal pulse shapers materials (copper and aluminum), the inflection point T_1 becomes smaller as the thickness increases. This is due to the compressive strength of the pulse shaper material has a strain rate effect, but the effects on the inflection point T_1 are much smaller than the pulse shaper diameters. For the non-metallic material pulse shapers (nylon and rubber), with the increase of pulse shaper thicknesses, the height of the inflection point T_1 basically remains unchanged, but the time to reach the inflection point T_1 gradually increases, i.e., the duration of loading area I gradually increases. It is worth noting that for rubber pulse shapers with thicknesses of 0.8mm and 1.0mm, the incident waveforms coincide with each other, which shows that rubber material is limited in thickness as a pulse shaper. In other words, when the rubber pulse shaper thickness is less than a certain value, the shaper is not applicable.

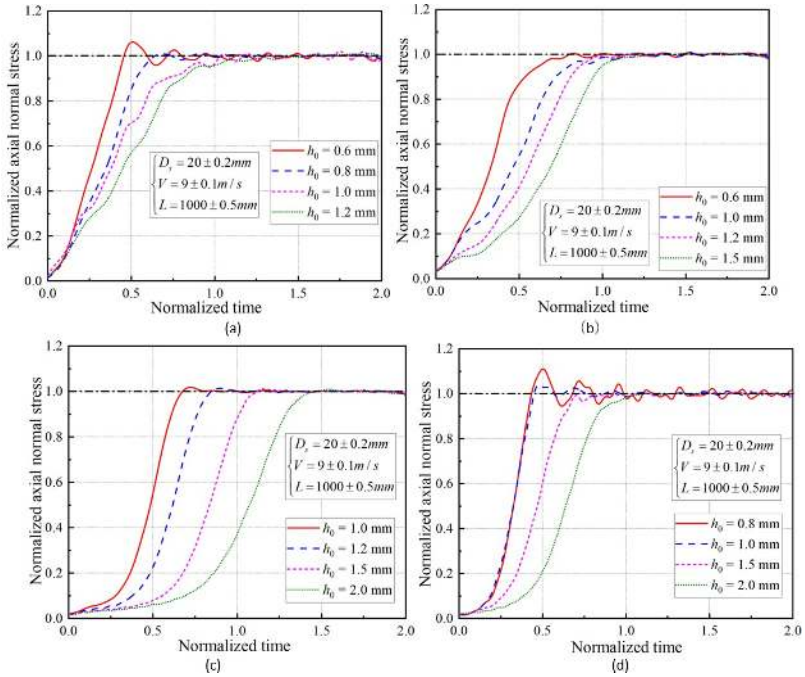


Figure 6 Incident curves of four pulse shaper materials with different thicknesses after shaping:(a) copper; (b) aluminum; (c) nylon; (d) rubber.

Regarding the effect of the pulse shaper dimensions on the incident pulse, Frew et al. (2001, 2002) performed a series of experiments on a shaper with a copper material. Based on the material volume incompressibility and uniform deformation theory, the theoretical model of the shaper affecting the incident wave is obtained.

$$\sigma_i(t)=\frac{a}{A_b}\frac{\sigma_s g(\varepsilon_p)}{(1-\varepsilon_p)} \tag{9}$$

where σ_s, ε_p and $g(\varepsilon_p)$ are the compressive strength, engineering strain and engineering strain functions of the pulse shaper, respectively.

The pulse shaper thickness on the incident waveform mainly affects ε_p in **Eq. (9)**, i.e., with the engineering strain of pulse shaper material increasing, the inflection point T_2 will be closer to the right. The engineering strain ε_p has the following relationship with the pulse shaper thickness.

$$\varepsilon_p = \frac{\Delta h}{h_0} = \frac{h_0 - h_f}{h_0} \tag{10}$$

where h_f , h_0 and Δh are the current thickness, initial thickness and thickness variation of the shaper, respectively.

The pulse shaper thicknesses after the experiment were measured as shown in **Table 3. Fig. 7** shows the variation of engineering strain with thickness h_0 for different pulse shaper materials. As the original pulse shaper thickness decreases, the thickness of copper, aluminum and rubber after the experiment also decreases, while for the nylon material, the pulse shaper thickness after the experiment remains unchanged. The engineering strain change of copper, aluminum and nylon pulse shapers after the experiments are consistent with the inflection point T_2 of the incident pulse. The inflection points T_2 of incident pulse with the thickness of 1.0mm and 1.2 mm of copper pulse shaper are approximately the same as shown in **Fig. 6 (a)**, which is consistent with the engineering strain change of copper pulse shaper. For the rubber shaper material, the engineering strain and the inflection point of the waveform are inconsistent, which is determined by the nature of the rubber material.

Table 3 Thicknesses of different pulse shaper materials before and after experiment

Copper	h_0 (mm)	1.2	1.0	0.8	0.6
	h_f (mm)	0.68	0.56	0.46	—
Aluminum	h_0 (mm)	1.5	1.2	1.0	0.8
	h_f (mm)	0.50	0.40	0.36	0.30
Nylon	h_0 (mm)	2.0	1.5	1.2	1
	h_f (mm)	0.16	0.16	0.16	0.16
Rubber	h_0 (mm)	2.0	1.5	1.0	0.8
	h_f (mm)	1.64	1.2	0.74	0.7

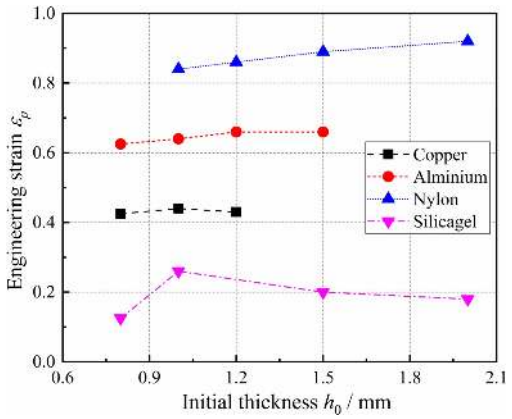


Figure 7 The engineering strain ε_p of different shaper materials with the change of h_0

3.3 The strike bar velocity

In SHPB experiment, the strain rate is related to the strike bar velocity. Generally speaking, the specimen strain rate is directly proportional to the impact velocity. In this paper, the effects of the strike bar velocities on the incident pulse were studied by copper pulse shaper with a diameter of 20mm and a thickness of 1mm. **Fig.8** demonstrates the incident pulse with different strike bar velocities when the same pulse shapers are used in SHPB experiment. Based on the experiment results, the incident pulse peak stress is increased by increasing the strike bar velocity, and the rise time of incident pulse is reduced.

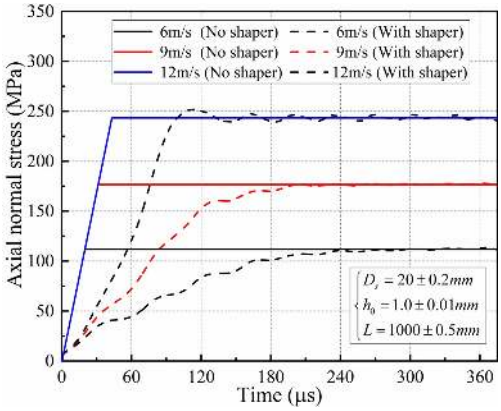


Figure 8 Incident pulse with different strike bar velocities

The inflection point T_1 also increases with an increase of the strike bar velocity. This is because the yield strength of pulse shaper material has a strain rate effect, which is essentially the increase of the material dynamic yield strength. The strain rate effect of pulse shaper material is not sensitive, resulting in the increase of inflection point T_1 is not obvious. The inflection point T_2 in the incident pulse gradually moves to the left with the strike bar velocity is increased, because the deformation of pulse shaper is related to the strike bar velocity. As the strike bar velocity increases, the deformation speed of pulse shaper material is accelerated, which results in the shortening of the plastic loading time in the incident pulse. The plastic loading area II in the waveform decreases, resulting in the left shift of inflection point T_2.

3.4 The strike bar length

According to the wave theory, the incident pulse duration is twice the propagation time of wave velocity in the strike bar. The duration of the incident pulse is increased when the strike bar length increases (**Fig. 9(a)**). For the identical pulse shaper dimensions and strike bar velocity, when the strike bar length changes from 500mm to 1000mm, the elastic loading area I and the plastic loading area II overlap. However, due to the excessive energy absorbed by the pulse shaper in SHPB experiment with the strike bar length of 500mm, the rigid loading part III and the partially plastic loading part II of the incident pulse are absorbed, but the total loading time remains unchanged, as shown in **Fig. 9(b)**.

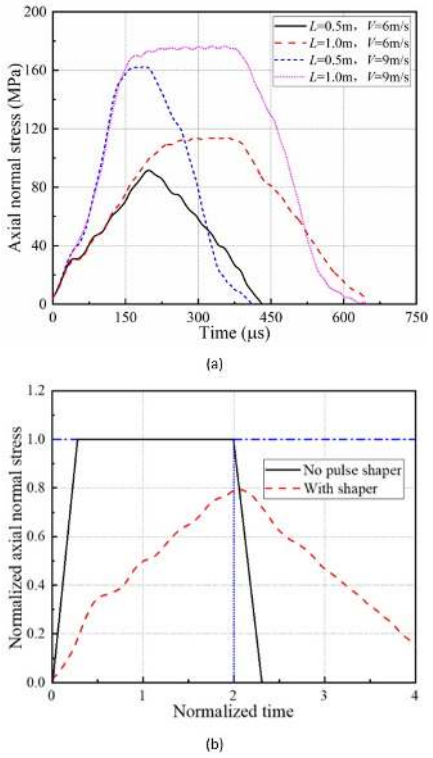


Figure 9 Strike bar lengths affect the incident pulse with aluminum shaper dimensions Ø20×1mm: (a) different lengths of strike bar; (b) the strike bar length is 500mm with or without pulse shaper.

4 Design of pulse shaper in SHPB experiment

For the brittle materials, the dynamic stress equilibrium (Vecchio and Jiang, 2007) and constant strain rate (Zhang et al., 2012) of the specimen are the prerequisites for ensuring the accuracy of the experiment results, which can be achieved by using an appropriate pulse shaper dimensions. In fact, the reflected pulse is the reflection of strain rate in SHPB experiment, so the influence factors of the incident pulse need to be applied to the reflected pulse. In SHPB experiment, the sum of the incident pulse and reflected pulse is equal to the transmitted pulse. When the strike bar velocity is constant, the stress-strain curve of concrete specimen is assumed to be constant, i.e., the transmitted pulse shape is unchanged. Therefore, the pulse shaping technique is to shape the reflected pulse by shaping the incident pulse. **Fig.10** is a schematic diagram of incident, reflected and transmitted pulse at different pulse shaper diameters and the identical strike bar velocities in SHPB. When the inflection point T_1 of the incident pulse increases, the initial inflection point of the reflected pulse is also increased. The pulse shaper thickness absorbs energy mainly through plastic deformation, making a plateau appears in the reflected pulse.

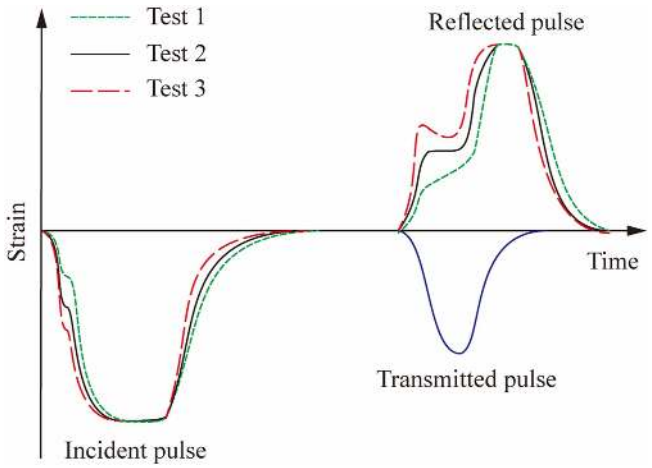


Figure 10 The schematic diagram of experimental results with different pulse shaper diameters (the pulse shaper thickness and strike bar velocity and its length are identical).

Fig.11 shows two typical non-constant strain rate reflected pulse and the corrected reflected pulse. Combined with the improved method of the pulse shaper on the reflected pulse, the reflected pulse can be achieved a constant strain rate by adjusting the shaper dimensions. For the first reflected pulse with the strain is increased gradually(**Fig.11**(a)), under the condition of constant impact velocity, it is necessary to increase the pulse shaper diameter to make the initial inflection point of the reflected wave larger, and increase the shaper thickness and absorb more energy so that the reflected wave becomes the waveform as shown in the red line in **Fig.11** (a). For the second reflected pulse with decreasing strain (**Fig.11**(b)), the pulse shaper diameter and thickness is too large, resulting in too high an initial inflection point and too much energy absorption. The pulse shaper diameter and thickness can be reduced to make it become the waveform shown in the red line in **Fig. 11**(b).

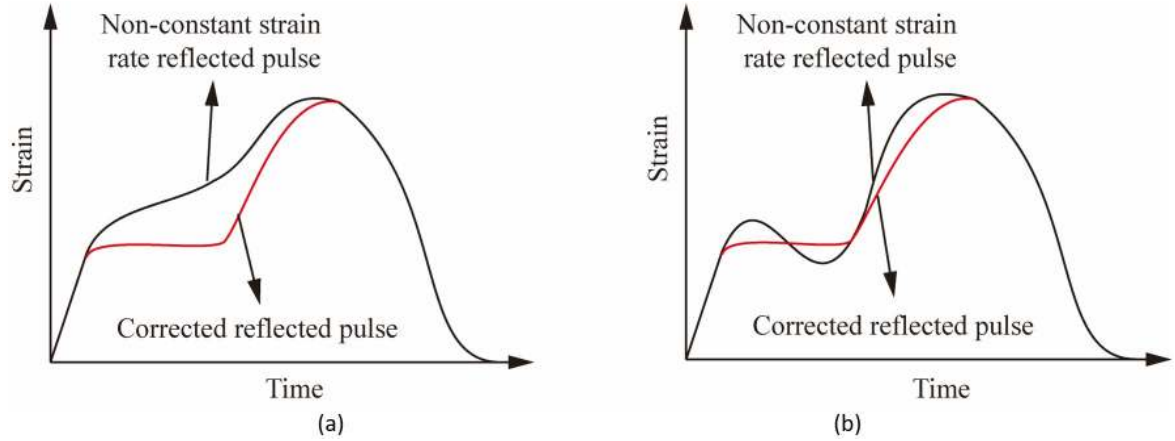


Figure 11 Two types of typical reflected and corrected pulse: (a) first type of reflected pulse; (b) second type of reflected pulse.

In the actual SHPB experiment, especially for specimen sensitive to the strain rate effect, it may not be possible to achieve the ideal loading conditions by changing the pulse shaper dimensions. In this case, the strike bar velocity needs to be adjusted to achieve constant strain rate loading. For the first reflected pulse, when the pulse shaper diameter and thickness increases, it is also necessary to reduce the strike bar velocity. The second reflected pulse increases the strike bar velocity while reducing the pulse shaper thickness and diameter.

To further study the effects of pulse shaper dimensions on achieving constant strain rate loading, this paper takes copper shaper as an example, employing different pulse shaper dimensions to perform several experiments on concrete. The concrete size is Ø68×34mm (length to diameter ratio is 0.5), and the quasi-static compressive strength is 51.6MPa. Also, the strike bar velocity and length are 9m/s and 500mm, respectively. According to the selection of pulse shaper for the brittle materials in the SHPB experiment, the pulse shaper dimensions is adjusted during the experiment. The experiment results of pulse shaper with sizes of $\text{Ø}32 \times 1.0\text{mm}$, $\text{Ø}38 \times 1.5\text{mm}$ and $\text{Ø}34 \times 1.2\text{mm}$ were obtained as shown in **Fig. 12**.

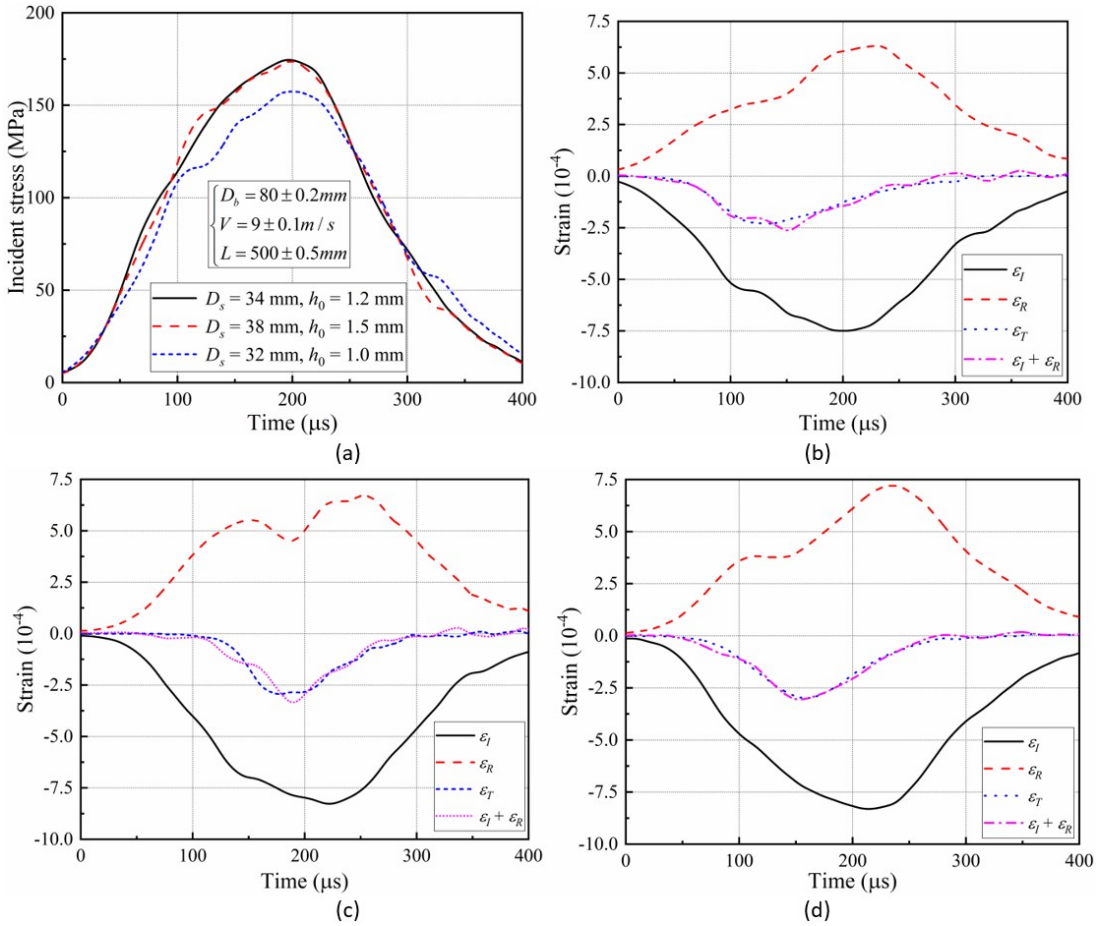


Figure 12 Concrete SHPB experimental results with (a) Incident pulse; dynamic equilibrium of using pulse shapers with (b) $\text{Ø}32 \times 1.0\text{mm}$; (c) $\text{Ø}38 \times 1.5\text{mm}$; (d) $\text{Ø}34 \times 1.2\text{mm}$.

The incident pulse of these experiments employing different pulse shaper dimensions are shown in **Fig. 12(a)**. After the pulse shaper is used, the high-frequency oscillation wave is filtered, and the rise time of the incident wave is prolonged. Because the failure strain of concrete in SHPB experiment is less than 1%, if the rise time of incident pulse is too short, the stress of concrete specimens will be inhomogeneous before failure, which does not satisfy the stress equilibrium assumption. To investigate the dynamic stress equilibrium, sum of the incident (ε_I) and reflected pulse (ε_R) is compared to the transmitted pulse (ε_T). Two pulses near the failure point of concrete specimen have a large difference as shown in **Fig. 12(b)** and **(c)**, which indicates that the stress is not balanced when the specimen is damaged during the experiment. For experimental results of pulse shaper with 34mm diameter and 1.2mm thickness (**Fig. 12(d)**), it is shown that two waveforms near the failure point of the specimen have good repeatability, which indicates that the stress equilibrium state is achieved before the specimen failure.

To accurately obtain the dynamic mechanical properties of the concrete material, it is necessary to maintain a constant strain rate when the concrete specimen is broken, i.e., the reflected pulse needs to have a platform segment, so that a constant strain rate can be obtained. **Fig. 13** is the strain rate as a function of time after three different shaper dimensions. It can be seen that the strain rate is approximately constant when the pulse shaper dimensions is Ø34×1.2 mm.

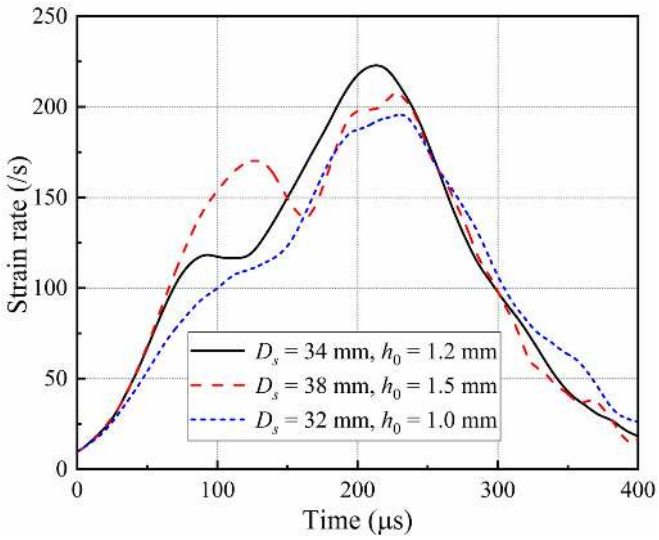


Figure 13. Strain rate curves of different pulse shaper dimensions

Fig. 14 shows the stress-strain curves of concrete after SHPB experiments with different pulse shaper dimensions. It can be seen that the non-constant strain rate has a great influence on the compressive strength. It is noteworthy that the compressive strength obtained by the pulse shaper dimensions of $Ø32 \times 1.0$ mm is quite different from that of $Ø34 \times 1.2$ mm. When the pulse shaper dimensions is $Ø38 \times 1.5$mm, the dynamic compressive strength is very close to the real compressive strength. It is shown when the strain rate of SHPB experiment for concrete is difficult to guarantee constant, the pulse shaper with larger thickness should be selected, and the experimental data obtained are less different from the real experimental. For the SHPB experiment of concrete material with pulse shaper, it is expected to obtain an incident pulse similar to the stress response of concrete., the effect of pulse shaper dimensions and strike bar parameters on the incident pulses have been discussed in section 3, which include the rigid loading stage. When it is necessary to generate an incident pulse similar to the stress response (transmitted pulse) of concrete, the rigid loading stage of incident pulse is eliminated, which can be realized by increasing the pulse shaper thickness to absorb more energy during the test.

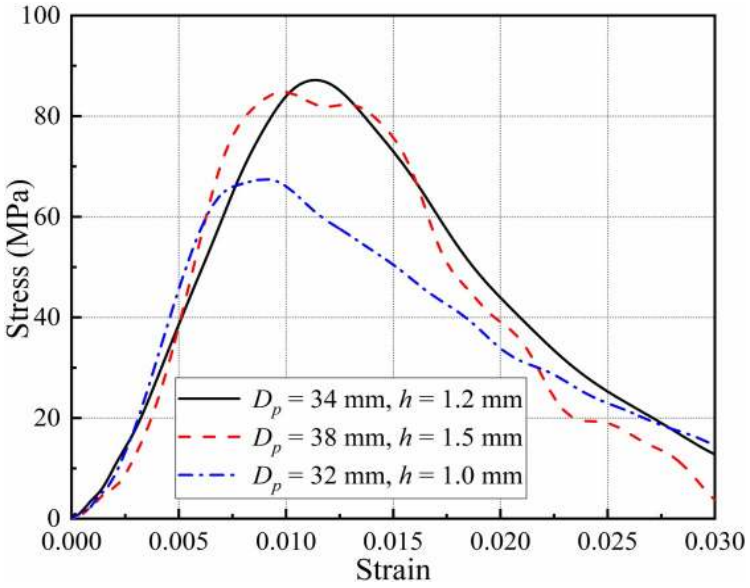


Figure 14 Stress-strain curves of different pulse shaper dimensions

5 CONCLUSIONS

In this paper, four kinds of pulse shaper materials on the incident pulse are studied by using 80mm SHPB apparatus. The main factors affecting the incident pulse include the pulse shaper thicknesses and diameters and the strike bar velocity and its length. On this basis, two typical non-constant reflected pulse and its improved methods in the SHPB experiment of brittle materials are analyzed. The SHPB experiment of concrete material is carried out by using the improved method. The dynamic stress equilibrium and constant strain rate loading under different pulse shaper dimensions are analyzed. The main conclusions are as follows:

(1) In the SHPB experiment, the pulse shaper can filter out the high-frequency oscillation wave and prolong the rise time of the incident pulse. By changing the pulse shaper dimensions, the incident pulse can be changed. For metal pulse shaper materials (copper and aluminum), the diameter mainly affects the first inflection point T_1 of the incident pulse and the elastic loading region I, i.e., the inflection point T_1 and loading area I gradually increase with the increase of pulse shaper diameters. For non-metallic materials (nylon and rubber), the pulse shaper diameter will not affect the inflection point T_1. But with the increase of diameter, the inflection point T_2 moves to the right gradually, and the duration of plastic loading area II becomes longer. The pulse shaper thickness mainly absorbs energy, which affects the duration of plastic loading area II. The difference of inflection point T_1 is that the pulse shaper strength has strain a rate effect. It is noteworthy that the use of rubber has a certain thickness and diameter limitations.

(2) The strike bar length and its velocity also affect the incident pulse. When the impact velocity is constant, the incident pulse duration increases with the strike bar length. When the strike bar length is constant, with the impact velocity increases, the duration of the incident pulse is unchanged, but the waveform rise time becomes shorter.

(3) An improved method for two typical reflected pulses in the SHPB experiment of concrete is obtained. When the reflected pulse is continuously reduced in the experiment, the pulse shaper diameter and thickness can be reduced. Instead, it requires increasing the pulse shaper diameter and thickness.

(4) In the SHPB experiment of concrete, the dynamic stress equilibrium and constant strain rate loading are necessary prerequisites for obtaining effective data. When the strain rate is not constant in the experiment, it has a great influence on the compressive strength. The constant strain rate loading can be achieved by using appropriate pulse shaper dimensions. For the SHPB experiment of concrete, it is recommended that the pulse shaper with larger thickness to make the rising time of the incident pulse longer and the loading stress slowly increase, so that the specimen can reach the stress equilibrium before failure.

Acknowledgements

The author discloses the receipt of the following financial support for the research, authorship, and/or publication of this article: The project was supported by the National Natural Science Foundation of China (Grant No: 11772160, 11472008,11802001), the Foundation of the State Key Laboratory of Explosive Science and Technology (Grant No: KFJJ18-01M), the Postgraduate Education Reform Project of Jiangsu Province (Grant No: KYCX18_0461).

Author's contributions: Conceptualization, J Wang, L Xu and G Gao; Methodology, J Wang, Z Du and G Gao; Investigation, J Wang, W Li and L Xu; Writing- original draft, J Wang, L Xu and G Gao; Writing - review & editing, G Gao and Z Du; Funding acquisition, G Gao and J Wang; Supervision, G Gao and Z Du; Data curation, J Wang, W Li and L Xu.

Editor: Marcílio Alves.

References

Bagher Shemirani, A., Naghdabadi, R. & Ashrafi, M. J. (2016), Experimental and numerical study on choosing proper pulse shapers for testing concrete specimens by split Hopkinson pressure bar apparatus, Construction and Building Materials, Vol. 125326-336.

Baranowski, P., Malachowski, J., Gieleta, R., Damaziak, K., Mazurkiewicz, L. & Kolodziejczyk, D. (2013), Numerical study for determination of pulse shaping design variables in SHPB apparatus, Bulletin of the Polish Academy of Sciences: Technical Sciences, Vol. 61 No. 2, pp. 459-466.

Chen, W., Lu, F., Frew, D. J. & Forrestal, M. J. (2002), Dynamic Compression Testing of Soft Materials, Journal of Applied Mechanics, Vol. 69 No. 3, pp. 214.

Chen, W., Song, B., Frew, D. J. & Forrestal, M. J. (2003), Dynamic small strain measurements of a metal specimen with a split Hopkinson pressure bar, Experimental Mechanics, Vol. 43 No. 1, pp. 20-23.

Chen, X., Wu, S. & Zhou, J. (2013), Experimental and modeling study of dynamic mechanical properties of cement paste, mortar and concrete, Construction & Building Materials, Vol. 47 No. oct., pp. 419-430.

Frew, D. J., Forrestal, M. J. & Chen, W. (2001), A split Hopkinson pressure bar technique to determine compressive stress-strain data for rock materials, Experimental Mechanics, Vol. 41 No. 1, pp. 40-46.

Frew, D. J., Forrestal, M. J. & Chen, W. (2002), Pulse shaping techniques for testing brittle materials with a split hopkinson pressure bar, Experimental Mechanics, Vol. 42 No. 1, pp. 93-106.

Frew, D. J., Forrestal, M. J. & Chen, W. (2005), Pulse shaping techniques for testing elastic-plastic materials with a split Hopkinson pressure bar, Experimental Mechanics, Vol. 45 No. 2, pp. 186-195.

Guo, Y. B., Gao, G. F., Jing, L. & Shim, V. P. W. (2017), Response of high-strength concrete to dynamic compressive loading, International Journal of Impact Engineering, Vol. 108114-135.

Heard, W. F., Martin, B. E., Nie, X., Slawson, T. & Basu, P. K. (2014), Annular Pulse Shaping Technique for Large-Diameter Kolsky Bar Experiments on Concrete, Experimental Mechanics, Vol. 54 No. 8, pp. 1343-1354.

Hwang, D. S., Rho, B. L. & Hong, S. I. (2005), A Study on the Dynamic Material's Characteristics of Tungsten Alloy using Split Hopkinson Pressure Bar, Journal of the American Ceramic Society, Vol. 64 No. 7, pp. 410–415.

Kolsky, H. (1949), An Investigation of the Mechanical Properties of Materials at very High Rates of Loading, Proceedings of the Physical Society B, Vol. 62 No. 11, pp. 676-700.

Li, X. B., Lok, T. S., Zhao, J. & Zhao, P. J. (2000), Oscillation elimination in the Hopkinson bar apparatus and resultant complete dynamic stress–strain curves for rocks, International Journal of Rock Mechanics and Mining Sciences, Vol. 37 No. 7, pp. 1055-1060.

Lok, T. S., Li, X. B., Liu, D. & Zhao, P. J. (2002), Testing and Response of Large Diameter Brittle Materials Subjected to High Strain Rate, Journal of Materials in Civil Engineering, Vol. 14 No. 3, pp. 262-269.

Ma, L., Li, Z., Liu, J., Duan, L. & Wu, J. (2019), Mechanical properties of coral concrete subjected to uniaxial dynamic compression, Construction and Building Materials, Vol. 199244-255.

Naghdabadi, R., Ashrafi, M. J. & Arghavani, J. (2012), Experimental and numerical investigation of pulse-shaped split Hopkinson pressure bar test, MATERIALS SCIENCE AND ENGINEERING A-STRUCTURAL MATERIALS PROPERTIES MICROSTRUCTURE AND PROCESSING, Vol. 539285-293.

Panowicz, R., Janiszewski, J. & Kochanowski, K. (2018), Influence of pulse shaper geometry on wave pulses in SHPB experiments, Journal of Theoretical and Applied Mechanics, 1217-1221.

Parry, D. J., Walker, A. G. & Dixon, P. R. (1995), Hopkinson bar pulse smoothing, Measurement Science and Technology, Vol. 6 No. 5, pp. 443-446.

Peroni, M., Peroni, L. & Avalle, M. (2006), High strain-rate compression test on metallic foam using a multiple pulse SHPB Apparatus, JOURNAL DE PHYSIQUE IV, Vol. 134609-616.

Su, H., Xu, J. & Ren, W. (2014), Mechanical properties of ceramic fiber-reinforced concrete under quasi-static and dynamic compression, MATERIALS AND DESIGN, Vol. 57 No. may, pp. 426-434.

Tang, Y., Sun, B., Ding, X. & Gu, B. (2008), Mechanical properties of 3-D glass/polyester resin cellular woven composite under impact loading, Pigment & Resin Technology, Vol. 37 No. 6, pp. 410-415.

Vecchio, K. S. & Jiang, F. (2007), Improved Pulse Shaping to Achieve Constant Strain Rate and Stress Equilibrium in Split-Hopkinson Pressure Bar Testing, METALLURGICAL AND MATERIALS TRANSACTIONS A-PHYSICAL METALLURGY AND MATERIALS SCIENCE, Vol. 38 No. 11, pp. 2655-2665.

Xin, L., Xu, J. Y., Bai, E. L. & Li, W. (2013), Research on the dynamic compressive test of highly fluidized geopolymer concrete, Construction & Building Materials, Vol. 48 No. nov., pp. 166-172.

Yang, H., Song, H. & Zhang, S. (2015), Experimental investigation of the behavior of aramid fiber reinforced polymer confined concrete subjected to high strain-rate compression, Construction and Building Materials, Vol. 95 No. oct.1, pp. 143-151.

Zhang, X. X., Ruiz, G., Yu, R. C., Poveda, E. & Porras, R. (2012), Rate effect on the mechanical properties of eight types of high-strength concrete and comparison with FIB MC2010, Construction and Building Materials, Vol. 30p.301-308.